Preparation of Superhydrophobic Teflon® AF 1600 Sub-Micron Fibers and Yarns Using the Forcespinning™ Technique

Yatinkumar Rane[1], Aleksey Altecor[1], Nelson S. Bell[2], PhD, Karen Lozano[1]

[1]University of Texas Pan American, Edinburg, Texas UNITED STATES

[2]Sandia National Laboratory, Albuquerque, New Mexico UNITED STATES

Correspondence to:
Karen Lozano email: lozanok@utpa.edu

ABSTRACT

Superhydrophobic materials combined with manufacturing processes that can increase surface roughness of the material, offer an opportunity to effectively control wetting properties. Rapid formation of Teflon® AF (TAF) fibrous mats with sub-micron fiber diameter using the Forcespinning™ technique is presented. The fiber formation technique is based on the use of centrifugal forces. SEM analysis shows uniform formation of TAF 1600 fibers with average diameter of 362±58nm. Contact angle measurement confirms the superhydrophobic nature of the mats with contact angles as high as 169° ± 3° and rolling angles of 2°. TAF 1600 mats were forcespun at a rate of 1gr/min. The relationship between the contact angle and hierarchical surface roughness of the TAF mat is also discussed. TAF yarns were also manufactured and characterized. Yarns with diameters of 156 microns withstood 17.5 MPa of engineering stress with a Young's modulus of 348 MPa in the elastic region and excellent thermal stability.

Keywords: Teflon®, Forcespinning™, superhydrophobic nanofibers, nanofiber yarns.

INTRODUCTION

Over the last few decades, research in super-hydrophobicity [1-6] (contact angle >150°) has attracted much attention given its potential applications, such as antifouling and self-cleaning structures, anti-icing coatings, stain-resistant textiles and in microfluidic devices [7-10]. Superhydrophobic surfaces are easily found in nature and typified by the lotus leaf (*Nelumbo nucifera*). Barthlott and Neinhuis [11] performed a systematic analysis of the lotus leaf and reported that the surface decoration on the leaf produced by a combination of epicuticular wax crystals and micro-scale papillae imparts water repellency and self-cleaning properties. Trying to reproduce the "lotus effect", researchers have developed superhydrophobic surfaces by engineering low surface energy materials using techniques such as etching, [12,13] templating, [14,15] and electrospinning [2,16]. In electrospinning [17,18], nano-fiber mats are developed when a polar solution is subjected to a strong electric force that induces a counter force to the surface tension, therefore leading to the production of a thin polymer jet. This jet dries rapidly in transit to a grounded target producing nanofibers.

Roughness introduced by sub-micron fiber morphology increases the wetting contact angle (CA) [7]. Studies indicate that a combination of low surface energy and surface roughness are the main requirements to obtain superhydrophobicity. Zisman [19] explains in a classic review the fundamentals regarding the wettability of low- and high-energy solid surfaces. The effect of surface roughness on hydrophobicity has been established by Wenzel [20] in Eq. (1), and Cassie and Baxter [21] in Eq. (2):

$$\cos\theta_W = r\cos\theta_Y \quad (1)$$

$$\cos\theta_{CB} = -1 + f(1 + \cos\theta_Y) \quad (2)$$

In Wenzel's equation, r is a roughness factor which is a ratio of the actual area of a rough surface to the flat projected area and θ_Y is Young's CA. The roughness increases the extent of contact between the surface and the liquid in smaller apparent area and results in a higher CA. However, the roughness factor is always greater than 1 and therefore the Wenzel's equation yields increased CA only for hydrophobic surfaces, i.e. for $\theta_Y > 90$, while the opposite is observed for hydrophilic surfaces, i.e. $\theta_Y < 90$. In the Cassie-Baxter's equation, f represents the fraction of

the liquid-solid contact area where the solid is a heterogeneous surface composed of solid and air. Thus, the liquid droplet sits on the textured surface with trapped air in-between the texture and therefore exhibits higher CA.

The development of superhydrophobic materials with improved mechanical and thermal performance promotes potential improvements in many applications [22]. As the scope and challenges of modern technology expand to include increasingly harsh environments, the engineering solutions enabling the desired performance can quickly become cost-prohibitive. Superhydrophobic nanofiber-derived surfaces stand as a prime route for this purpose due to their ability to capitalize on the material's active properties. It is thus easy to envision protective barriers and coatings for structures small and large that extends the operable ranges into further extremes of corrosion, fouling, temperature, and time.

Fluoropolymers are excellent materials to obtain superhydrophobicity given its characteristic low surface energy. Teflon®AF (TAF), an amorphous fluoropolymer, is a copolymer of perfluorodimethyl dioxole (PDD) and tetrafluoroethylene (TFE) and exhibits excellent mechanical properties, chemical resistance, low refractive index, and the lowest dielectric constant (1.89-1.93) of any plastic. These characteristics come from the C-F bond which is termed as the strongest bond in organic chemistry. The presence of PDD in TAF makes this polymer soluble in certain perfluorinated solvents [23-25]. Due to the above mentioned properties, numerous attempts have been conducted to produce nano/ sub-micron TAF fibers to increase its super-hydophobicity. Nonetheless, the characteristic low dielectric constant of TAF makes it difficult to dissolve in a sufficiently polar solvent which inhibits the response towards applied electric forces for conventional electrospinning processes [26-28]. The semicrystalline polytetrafluoroethylene (PTFE) has a high melt viscosity (~10^{11} poise at 380 °C) and is non-soluble in many solvents which makes it difficult to electrospin in addition with its low dielectric constant properties [29,30]. Researchers have therefore used sacrificial polymers such as polyvinyl alcohol (PVA), [31,32] or polyethylene oxide (PEO) to electrospin PTFE fibers [33]. The subsequent heat treatment to remove sacrificial polymer has resulted in the loss of fiber morphology. The TAF polymers are soluble only in certain perfluorinated solvents and reported as non-electrospinnable. Although, it has been reported that coaxial fibers can be formed with the help of an electrospinnable core [26] or sheath [27]. Scheffler et al. [28] reported electrospinning of TAF 1600 fibers, however, they observed that the process was not steady and formed non-uniform fiber morphology of the TAF 1600 micron size fibers.

This work demonstrates a steady and direct route for the preparation of TAF 1600 nano/sub-micron fibers using the Forcespinning™ (FS) approach. This ultimately advances Teflon into more wide-spread applications as a protective agent. The fibers were collected as a free standing mat and characterized for hydrophobic properties. Additional samples were then also processed into yarns of varying diameters and degrees of twist. FS is a technique that can produce nano to micron size fibers from a broad range of materials such as polymers, metals, ceramics, and composites [34-37]. One of the features of this technique is the high yield of at least 1 g/min in the laboratory prototype (versus 0.3grams/hr in an electrospinning laboratory instrument). *Figure 1* shows a schematic of the FS setup. Briefly, a spinneret is mounted on a shaft which is connected to an electric motor. In this way, the applied centrifugal force is mainly responsible to drive the material through a designed set of orifices

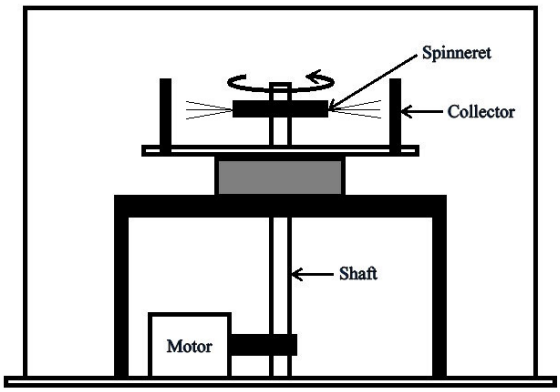

FIGURE 1. Schematic of the Forcespinning™ bench top instrument.

on the spinneret to produce the fibers. The collector system gives the flexibility to collect fibers either as a free standing mat, to deposit fibers on a substrate, or to prepare 3D configurations. The processing variables that play an important role in the FS process are spinneret design, angular velocity and aerodynamics of the chamber.

EXPERIMENTAL

TAF 1600, a copolymer of 2,2-bis(trifluoromethyl)-4,5-difluoro-1,3-dioxole (65% mole) and 1,1,2,2,-tetrafluoroethylene, powder was obtained from

DuPont (Wilmington, DE). Fluorinert FC-40 (mixture of 1,1,2,2,3,3,4,4,4-nonafluoro-N,N-bis(1,1,2,2,3,3,4,4,4-nonafluorobutyl)-1-Butanamine, with 1,1,2,2,3,3,4,4,4-nonafluoro-N-(1,1,2,2,3,3,4,4,4 - nonafluorobutyl) -N- (trifluoromethyl) -1-butanamine) fluid was purchased from 3M Specialty Chemicals (St. Paul, MN) and used as received to dissolve the TAF powder. A solution of 10 wt% TAF 1600 in Fluorinert FC-40 was prepared by mixing the dry polymer powder into the solvent, and heating at 50 °C in a sealed container to prevent solvent loss through evaporation. Manual agitation was intermittently used to aid in homogenizing the solution. A uniform clear and transparent solution was formed after 24 hours, and the solution was used after three days storage at 50 °C to ensure uniformity of the dissolved polymer. The 10 wt% polymer concentration in the equilibrated solution was confirmed by thermogravimetric analysis.

The TAF 1600 solution was fed in a dual orifice spinneret and was rotated at varying revolutions per minute (rpm) ranging from 5,000 to 10,000 rpm. The optimum speed was found to be 8,000 rpm. Experiments were carried out using orifices with inner diameters of 241 micron, 191 micron, and 140 microns. The collector distances varied between 7 and 15 cm. All experiments were carried out in a closed chamber. The forcespun fibers were collected on a clean glass slide and annealed at 170 °C (T_g = 165 °C) for 105 minutes. The fiber morphology was studied using a Zeiss Sigma VP scanning electron microscope (SEM). Average diameters were calculated by measuring 200 fibers per sample.

Hydrophobicity of the annealed fibrous mat was found by CA measurements. Using a syringe with 30 gauge needle (I.D 140 μm), a drop of about 4-5 μL of deionized water was placed onto the TAF mat deposited on a glass slide and an image was captured with a digital camera. A light source covered with a diffuser was kept behind the substrate to obtain a clear image showing droplet contour and baseline. Five photos of droplets were analyzed by the DropSnake plug-in (A. Stalder, G. Kulik, D. Sage, L. Barbieri, P. Hoffman, C Colloid Surf. A-Physicochem. Eng. Asp. 2006. 286, 92) for ImageJ (W. S. Rasband, National Institutes of Health, Bethesda, MD, USA) to calculate the water CA. The rolling angle measurements were based on the procedure described by Muthiah et al.[27] The mats were tilted at certain angles and a drop (4-5 μL) of deionised water was released from a 4 mm height. The angle was noted as the droplet rolls-off completely from the mat. For each mat, three measurements were averaged.

Fibers intended for yarning were collected in 4x8 inch sheets of ¼ inch steel wire mesh. Teflon yarns were prepared in paired sets from the same batches of nanofibers: Set A was yarned after annealing while Set B was yarned immediately after spinning and annealed in its yarn form alongside the Set A fibers in a mat. Nanofibers were spun from the produced sheets into yarns at around 700 rpm for 5 to 45 seconds, producing twisted yarn lengths of 10 to 30 cm with varying degrees of twist. Thermal and mechanical properties of each set of yarns were studied using a TA Instruments TMA 2940 and DMA Q800, respectively. For mechanical analysis, yarns of 15 mm in length were cut into two pieces – a 5 mm length was examined in the SEM under environmental conditions to measure the yarn's diameter and degree of twist, while the remaining 10 mm was placed in the tension film/fiber clamp of the DMA to produce the stress-strain curves.

RESULTS AND DISCUSSION

The FS technique uses centrifugal forces for the production of fibers. As the spinneret is rotated at an angular velocity, a thin polymer jet is ejected from the orifice and continues to thin out as it travels in a spiral path before reaching the collector. The spinneret used in this work was a cylindrical tube. The exiting polymer jet undergoes a large pressure drop at the orifice followed by strong extensional and shear forces, which results in fiber formation through deformation, extension, and reorientation of the polymer chains. *Figure 2* shows the morphology of forcespun fibers at various conditions.

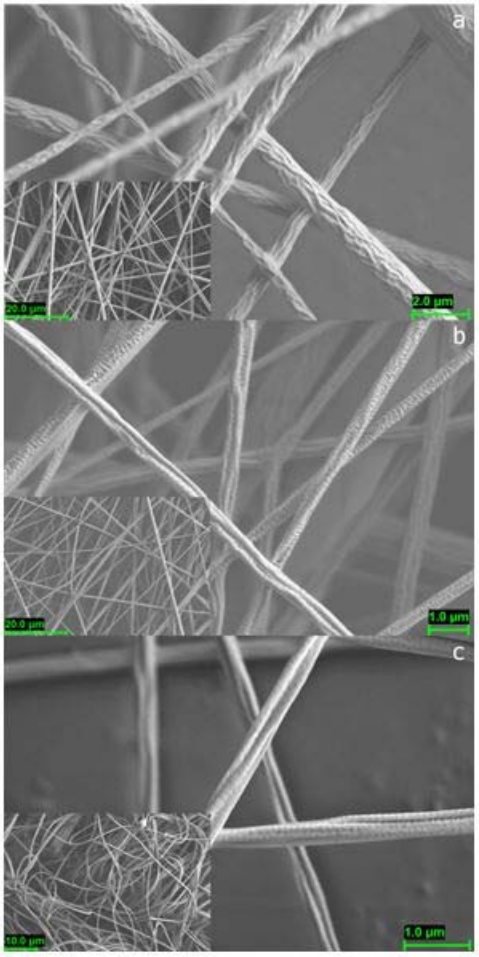

FIGURE 2. SEM micrographs of the TAF 1600 fibers forcespun with orifices of (a) 241 micron, (b) 191 micron, and (c) 140 micron. Each insert shows the corresponding lower magnification micrograph.

The fiber formation of TAF 1600 was stable and uniform as can be seen from inset micrographs shown in *Figure 2*. As the orifice dimensions reduced from 241 micron to 140 micron, the fiber diameter was decreased from 826±226 nm to 362±58 nm respectively (*Table I*).

TABLE I. Effect of FS Parameters on Fiber Diameter, Contact Angle, and Rolling Angle of TAF 1600 Fibrous Mats.

Orifice dim. (µm)	Angular velocity (rpm)	Fiber diameter (nm)	Collector distance (cm)	Contact angle (°)	Rolling angle (°)
241	8000	826±226	7	156±3	4±1
191	8000	673±137	7	162±2	2±1
140	8000	362±58	15	169±3	2±1
		TAF 1600 Film		113±1	>15

The fiber formation with 140 micron orifice and 7 cm collector distance yielded uneven surface morphology containing long beads and fiber networks (results not shown). Upon increasing the collector distance from 7 cm to 15 cm fibers were able to form a spiral path therefore promoting further extensional flow/evaporation and long homogeneous fibers were developed. *Figure 2a* shows the forcespun TAF 1600 fibers with 241 micron orifice with wrinkled and collapsed morphology on the fiber surface. The TAF 1600 fibers forcespun with 191 micron and 140 micron showed distinctive stretching in the wrinkled morphology in addition to a porous structure. This phenomenon indicates that the amount of extensional force increases with decreasing dimension of the polymer jet exiting from the spinneret orifice resulting in a long stretched surface texture on the fiber. The trend in the hierarchical surface morphology could be attributed to slower evaporation of the Fluorinert FC-40 solvent (T_b=165 °C). However, this characteristic surface morphology did not destroy the fiber formation. From the point of hydrophobicity, this type of texture is highly desired. Similar surface morphology is reported with TAF 1600 fibers [26, 28].

The solvent evaporation phenomena leading to polymer solidification and eventual formation of fiber morphology in FS is analogous to that of the electrospinning process except for a major parameter: the polymer jet carries a charge in the latter process. It is known that the fiber surface morphology depends on the rate of solvent evaporation. Koombungse et al. [38] have reported that electrospun fibers tend to form a mechanically distinct skin layer on the polymer jet due to rapid evaporation of the solvent which collapses once the internal solvent escapes and forms characteristic fiber shapes, including ribbons and wrinkled surfaces. The various shapes could be attributed to a thermally induced phase separation mechanism which occurs at the fiber surface due to evaporative cooling. Pai et al. [39] and Megelski et al. [40] reported porous structures in electrospun amorphous polymers such as polystyrene, polycarbonate, and polymethylmethacrylate using solvents with varying rates of evaporation. They proposed that the mechanism for the formation of porous structure with slow rate of solvent evaporation could be explained by vapor-induced phase separation. In this phase separation water vapor from the air penetrates into the polymer jet which leaves its imprint after complete evaporation resulting into porous structures. These hypotheses could explain the surface morphology of forcespun TAF 1600 fibers.

Superhydrophobic properties result from a combination of low surface energy and high surface roughness. *Table I* shows water CAs and rolling angle on the forcespun TAF 1600 fibers. All mats showed superhydrophobicity, exhibiting CA of more than 150°. The fibers forcespun with 140 micron orifices exhibited CA of 169° and rolling angle of 2°. The CA increased from 156° to 169° as the fiber diameter was decreased from 826 nm though 362 nm. Similar trend was also demonstrated by Ma et al.,[41] who reported that the decrease in fiber diameter introduces a higher level of roughness and therefore higher CA. Additionally, a second level of roughness (due to wrinkling) with the developed porous texture increased the number of air pockets in the mat resulting in higher CA according to the Cassie-Baxter model. For comparison, the TAF 1600 solution was cast into a film and processed in a similar way to that of forcespun fibers. The CA results obtained on the TAF film (113°) suggest that Wenzel's state is dominant on the relatively smooth film surface when compared to the composite surface (roughness imparted by sub-micron fibers) of the mats, where Cassie-Baxter state explains the mechanism for the experimented superhydrophobicity.

Yarns made of TAF fibers (shown in *Figure 3*) were prepared under two conditions, Set A, fibers annealed and yarned and Set B fibers yarned prior to annealing. *Table II* shows characteristics of the yarns. In both cases, it was observed that a degree of twist higher than 3000 turns per meter (tpm) was difficult to achieve due to several mechanical factors. During the yarning of Set B, the slightly uneven distribution of fibers over the source mat resulted in the creation of points of necking which contained slightly fewer fibers and were thus weaker and more susceptible to twisting than the thicker parts of the yarns. Although yarns without these weak points had been produced, they generally limit the amount of twist on a single yarn to roughly 10 seconds of twisting or 3000 tpm. Yarning of Set A fibers presents a different issue – the lack of any residual solvent (increase surface roughness) and resulting higher stiffness causes them to unwind once released from either end.

TABLE II. Typical properties of TAF yarns.

Yarn code	Diameter (μm)	Turns per meter (tpm)	Linear density (denier)
Set A	59-268	3000	~1030
Set B	175-462	3000	~680

Figure 4 documents the observed thermal (a) and mechanical (b) properties of the yarns. The thermal expansion coefficient was calculated to be 7.3×10^{-5} $°C^{-1}$ in the range from room temperature to 130 °C, where glass transition effects become significant. The calculated ultimate tensile strength (UTS) was 17.5 MPa for samples of Set B vs. 7 MPa for samples of Set A.

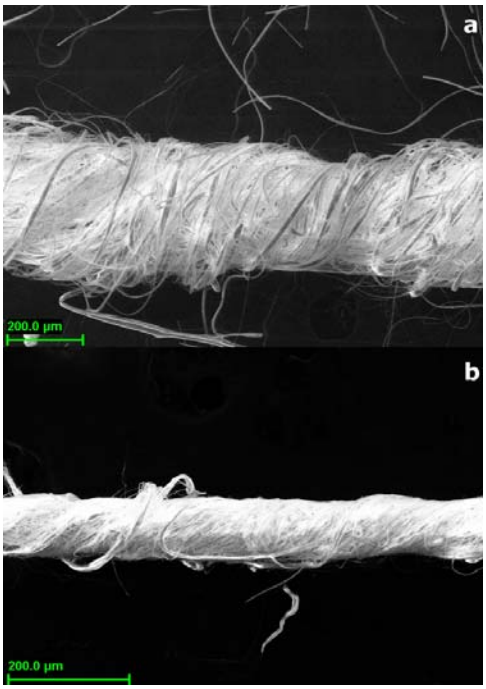

FIGURE 3. SEM micrographs of TAF 1600 yarns yarned (a) after annealing (Set A) and (b) before annealing (Set B).

Another significant difference between the two types of yarns is the two-stage nature in which Set A deformed, first in a linear high-strain fashion, followed by non-linear high-stress plastic deformation up to their failure point. This phenomenon is perhaps best explained by unwinding behavior – the loose yarns must first be returned to their tightened condition before any elastic or plastic deformation can take place, a point of much further strain since these fibers were pre-stretched during the yarning process and were not allowed additional relaxation from further annealing. Thus, the initial low-stress linear region of Set A samples exhibits a Young's modulus of just 211 KPa, which abruptly changes to a much higher 18.5 MPa with the onset of plastic deformation. Set B samples exhibit a higher and more consistent modulus of 348 MPa. In both cases, the thinner yarns were able to withstand higher levels of deformation prior to failure; the expectant direct relationship between degree of twist and UTS does not appear to be present in Set A, but clearly improves performance in Set B.

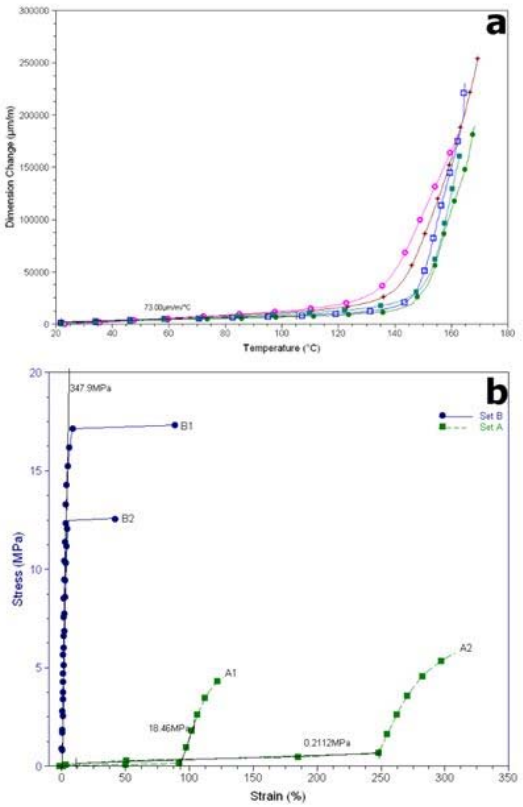

FIGURE 4. (a) Thermal and (b) mechanical properties of yarns. Dimensional properties in µm diameter and turns per meter of yarns as labeled in (b): A1 - 264 and 2700, A2 - 174 and 1750, B1 - 156 and 2500, B2 - 222 and 1700.

Thermal expansion, meanwhile, is unaffected by any of these factors and is simply a property of the constituent PTFE polymer, showing little variance between all samples.

CONCLUSION

Superhydrophobic TAF 1600 fibrous mats were prepared using the FS technique. The SEM analysis revealed homogeneous long fibers with uniform fiber size distribution. The TAF 1600 fibers forcespun with 140 micron orifices exhibited CA of 169° and rolling angle of 2° (average fiber diameter of 362±58 nm). Owing to the intrinsic physicochemical properties of the TAF polymer, the mats can perform in extreme weather conditions. Further, monolithic TAF fibers would preserve the superhydrophobic performance and life of the mats. Potential deployments of such fibers include anti –icing and -fouling coatings, while their yarned form is a viable option for structural applications with need of superior environmental stability. Additionally, the high yield offered by the FS technique also makes these fibrous mats and yarns interesting from the commercial point of view.

REFERENCES

[1] Nakajima, A.; Hashimoto, K.; Watanabe, T.; Recent studies on super-hydrophobic films; *Mon Chem.* 2001, *132*, 31.

[2] Ma, M.; Hill, R. M.; Superhydrophobic surfaces; *Current Opinion in Colloid & Interface Science* 2006, *11*, 193.

[3] Nosonovsky, M.; Bhushan, B.; Roughness-induced superhydrophobicity: a way to design non-adhesive surfaces; *Journal of Physics: Condensed Matter* 2008, *20*, 225009.

[4] Feng, X.; Jiang, L.; Design and creation of superwetting/antiwetting surfaces; *Advanced Matter* 2006, *18*, 3063.

[5] Guo, Z.; Liu, W.; Su, B.; Superhydrophobic surfaces: From natural to biomimetic to functional; *Journal of Colloid and Interface Science* 2011, *353*, 335.

[6] Blossey, R.; Self-cleaning surfaces – virtual realities; *Nature: Materials* 2003, *2*, 301.

[7] Ma, M.; Hill, R.; Rutledge, G.; A review of recent results on superhydrophobic materials based on micro- and nanofibers; *Journal of Adhesion Science and Technology* 2008, *22*, 1799.

[8] Meuler, A.; et al.; Relationships between water wettability and ice adhesion; *ACS Applied Materials & Interfaces* 2010, *2*, 3100.

[9] Gao, Y.; et al.; Novel water and oil repellent POSS-based organic/inorganic nanomaterial: Preparation, characterization and application to cotton fabrics; *Polymer* 2010, *51*, 5997

[10] Karuwan, C.; et al.; Tuantranont, Electro-chemical detection on electrowetting-on-dielectric digital microfluidic chip; *Talanta* 2011, *84*, 1384.

[11] Barthlott, W.; Neinhuis, C.; Purity of the sacred lotus, or escape from contamination in biological surfaces; *Planta* 1997, *202*, 1.

[12] Woodward, I.; et al.; Super-hydrophobic Surfaces Produced by Plasma Flourination of Polybutadiene Films; *Langmuir* 2003, *19*, 3432.

[13] Qian, B.; Shen, Z.; Fabrication of super-hydrophobic surfaces by dislocation-selective chemical etching on aluminum, copper, and zinc substrates; *Langmuir* 2005, *21*, 9007.

[14] Shirtcliffe, N.; et al.; Dual-Scale Roughness Produces Unusually Water-Repellent Surfaces; *Advanced Materials* 2004, *16*, 1929.

[15] Oner, D.; McCarthy, T.; Ultrahydrophobic Sur-faces: Effects of Topography Length Scales on Wettability; *Langmuir* 2000, *16*, 7777.

[16] Ma, M.; et al.; Electrospun Poly(Styrene-block-dimethylsiloxane) Block Copolymer Fibers Exhibiting Superhydrophobicity; *Langmuir* 2005, *21*, 5549.

[17] Renekar, D.; Chun, I.; Nanometre diameter fibres of polymer, produced by electrospinning; *Nanotechnology* 1996, *7*, 216.

[18] Renekar, D.; et al.; Bending instability of electrically charged liquid jets of polymer solutions in electrospinning; *Journal of Applied Physics* 2000, *87*, 4531.

[19] Zisman, W.; Relation of the Equilibrium Contact Angle to Liquid and Solid Constitution; *Advances in Chemistry Series* 1964, *43*, 1.

[20] Wenzel, R.; Resistance of Solid Surfaces to Wetting by Water; *Industrial & Engineering Chemistry Research* 1936, *28*, 988.

[21] Cassie, A.; Baxter, S.; Wettability of porous surfaces; *Transactions of the Faraday Society* 1944, *40*, 546.

[22] Zhang, X.; et al.; Superhydrophobic surfaces: from structural control to functional application; *Journal of Materials Chemistry* 2008, *18*, 621-633.

[23] Resnick, P.; Buck, W.; in *Fluoropolymers 2: Properties*; Plenum Press, New York, 1999, Ch. 2.

[24] O'Hagan, D.; Understanding organofluorine chemistry. An introduction to the C–F bond; *Chemical Society Reviews* 2008, *37*, 308.

[25] Grampel. R.; Surfaces of fluorinated polymer systems; *Ph.D. thesis*; Technische Universiteit Eindhoven, 2002. ISBN 90-386-2863-3 accessed through http://alexandria.tue.nl/extra2/200211249.pdf

[26] Han, D.; Steckl, A. J.; Superhydrophobic and Oleophobic Fibers by Coaxial Electrospinning; *Langmuir* 2009, *25*, 9454.

[27] Muthiah, P.; Hsu, S.; Sigmund, W.; Coaxially Electrospun PVDF-Teflon AF and Teflon AF-PVDF Core-Sheath Nanofiber Mats with Superhydrophobic Properties; *Langmuir* 2010, *26*, 12483.

[28] Scheffler, R.; Bell, N. S.; Sigmund, W.; Electro-spun Teflon AF fibers for Superhydrophobic Membranes; *Journal of Materials Research* 2010, *25*, 1595.

[29] Blanchet, T. A.; *Polytetrafluoroethylene, Handbook of Thermoplastics*; Marcel Dekker, NY, 1997.

[30] Burkarter, E.; et al.; Superhydrophobic electro-sprayed PTFE; *Surface and Coatings Techno-logy* 2007, *202*, 194.

[31] Xiong, J.; Huo, P.; Ko, F. K.; Fabrication of Ultrafine Fibrous Polytetrafluoroethylene Porous Membrane by Electrospinning; *Journal of Materials Research* 2009, *24*, 2755.

[32] Sijun, Z.; et al.; Preparation of Polytetrafluoro-ethylene Ultrafine Fiber Mats with Electro-spinning Process; *Materials Science Forum* 2011, *827*, 675.

[33] Anneaux, B.; Ballard, R.; Garner, D.; Electro-spinning of PTFE with High Viscosity Materials; *United States Patent Application* 20100193999 A1, 2010.

[34] Sarkar, K.; et al.; Electrospinning to Force-spinning™; *Materials Today* 2010, *13*, 12.

[35] Padron, S.; et al.; Production and characteriza-tion of hybrid BEH-PPV/PEO conjugated polymer nanofibers by Force-spinning™; *Journal of Applied Polymer Science* 2012, *125-5*, 3610-3616.

[36] McEachin, Z.; Lozano, K.; Production and characterization of polycaprolactone nanofibers via Forcespinning™ technology; *Journal of Applied Polymer Science* 2012, DOI: 10.1002/app.36843.

[37] Altecor, A.; Mao, Y.; Lozano, K.; Large-scale synthesis of tin-doped indium oxide nanofibers using water as solvent; *Functional Materials Letters* 2012, *5-3*, 120020.

[38] Koombhongse, S.; Liu, W.; Reneker, D.; Flat polymer ribbons and other shapes by electrospinning; *Journal of Polymer Science Part B: Polymer Physics* 2001, *39*, 2598.

[39] Pai, C.; Boyce, M.; Rutledge, G.; On the Mor-phology of Porous and Wrinkled Fibers of Polystyrene Electrospun from Dimethyl-formamide; *Macromolecules* 2009, *42*, 2102.

[40] Megelski, S.; et al.; Micro- and Nanostructured Surface Morphology on Electrospun Polymer Fibers; *Macromolecules* 2002, *35*, 8456.

[41] Ma, M.; et al.; Decorated Electrospun Fibers Exhibiting Superhydrophobicity; *Advanced Materials* 2007, *19*, 255.

AUTHORS'ADDRESSES
Yatinkumar Rane
Aleksey Altecor
Karen Lozano
University of Texas Pan American
1201 W University Dr
Edinburg, Texas 78539
UNITED STATES

Nelson S. Bell, PhD
Sandia National Laboratory
1515 Eubank
Albuquerque, New Mexico 87123
UNITED STATES